EUROPEAN MECHANICAL SCIENCE

Research Article

e-ISSN: 2587-1110

Fatigue analysis of 3D-printed polymer materials under various manufacturing parameters utilizing poisson regression method and ANOVA

Murat Horasan[1*], **İsmail Saraç**[1]

[1] Department of Mechanical Engineering, Aksaray University, Aksaray, Türkiye

Abstract: In this study, we conducted a statistical evaluation of the experimental results from a prior investigation by the authors concerning the fatigue behavior of 3-Dimensional (3D) printed Polylactic Acid (PLA) materials. Stress versus number of cycles (S-N) curves for the sample types were derived using the Poisson regression method. Within the scope of the statistical analysis, we performed average effect plots and an analysis of variance. At the conclusion of the study, we clearly observed the impact of printing parameters on the fatigue of 3D printed PLA materials, especially at low stress amplitude levels. At high stress amplitude values, the effect of printing parameters on the fatigue behavior of 3D printed PLA parts was limited. The analysis revealed that the stress level was the most influential factor determining the number of cycles to failure. While the production parameters of the PLA specimen, such as raster angle and printing speed, significantly impacted the results at a low stress level of 9.13 MPa, their effect was much less pronounced at a higher stress amplitude of 18.25 MPa, where variations in the number of cycles to failure among different specimen types were minimal. The analysis determined that the optimal parameter combination for 3D printed PLA fatigue specimens was a printing speed of 20 mm/s, a raster angle of 30°, and a stress amplitude of 9.13 MPa. According to the analysis of variance results, the parameter that most significantly influenced fatigue life was the stress level, contributing 54.93%. Raster angle and printing speed contributed 14.52% and 4.19%, respectively. The Poisson regression method proved to be an effective tool for plotting S-N graphs.

Keywords: fatigue, PLA, Poisson Regression, ANOVA, raster angle, printing speed.

1. Introduction

Additive Manufacturing (AM), also known as 3D printing, offers significant advantages in industrial applications due to its design flexibility. Initially, the AM method was mainly used for prototype production, but it has been extensively applied across many industries, particularly in the biomedical, aerospace, and automotive sectors, in recent years [1-7]. The AM method encompasses various production technologies. Specifically, the FDM (Fused Deposition Modeling) method, based on material extrusion for producing thermoplastic polymer parts, has gained popularity because of its cost-effectiveness and simplicity [8-10].

The mechanical properties of parts produced by the FDM method depend directly on printing parameters and environmental conditions. Important FDM printing parameters include layer thickness, print speed, fill ratio, print orientation, raster angle, extruder temperature, and table temperature [11, 12]. Most of these parameters not only influence the mechanical properties but can also significantly alter fabrication durations. Therefore, using optimal parameters is crucial for cost efficiency.

Research on the impact of printing parameters on the mechanical properties of FDM-3D printed materials has included numerous studies conducted under static loading conditions [13-17]. Although studies on the mechanical properties of FDM-3D printed parts under variable loading conditions have started in recent years, their number is still lower compared to those conducted under static loading conditions. Afrose et

*Corresponding author:
Email: murathorasan@aksaray.edu.tr

Cite this article as:

Horasan, M., Saraç, İ. (2025). Fatigue analysis of 3D-printed polymer materials under various manufacturing parameters utilizing poisson regression method and ANOVA. *European Mechanical Science*, 9(3): 246-254. https://doi.org/10.26701/ems.1717687

History dates:

Received: 11.06.2025, *Revision Request*: 08.07.2025, *Last Revision Received*: 17.07.2025, *Accepted*: 04.08.2025

al. [18] investigated the fatigue strength of 3D-printed PLA parts through tensile fatigue tests conducted at print orientations of 0°, 45°, and 90°. In the tensile tests, the highest strength value was recorded at the 0° orientation, while the longest fatigue life was achieved at the 45° orientation in the fatigue tests. Saraç and Horasan [19] assessed the torsional strength of 3D-printed PLA polymers produced at various printing speeds and raster angles, discovering that the optimal load-carrying capacity was obtained at 30° and 60° raster angles, while the lowest was recorded at a 0° raster angle. The torsional load-carrying capacity improved significantly for specimens produced at a printing speed of 80 mm/s. Specifically, there was an 85% increase compared to those manufactured at 20 mm/s.

Azadi et al. [20] investigated the effect of horizontal and vertical print orientation on the fatigue performance of 3D printed PLA and ABS samples using rotary-bending fatigue tests. The study concluded that fatigue strength was superior in the horizontal printing direction.

Dadashi and Azadi [21] investigated the fatigue behavior of 3D printed PLA parts using rotary-bending fatigue tests, focusing on the effects of printing temperature, printing speed, and nozzle diameter. The study parameters included nozzle diameters of 0.2, 0.4, and 0.6 mm, printing speeds of 5, 10, and 15 mm/s, and printing temperatures of 180, 210, and 240 °C. The highest fatigue life was observed at a 0.2 mm nozzle diameter, 180 °C printing temperature, and 5 mm/s printing speed. Notably, the maximum fatigue life was achieved at the lowest level of each parameter.

Akhoundi and Ouzah [22] investigated the effect of various printing parameters on the fatigue behavior of 3D-printed PLA parts through rotary-bending fatigue tests and finite element studies. The parameters that significantly affect the fatigue strength of 3D-printed PLA parts were identified as filler ratio, nozzle temperature, and layer height, respectively.

In the study by Horasan and Sarac [23], the effects of stress amplitude, printing speed, and raster angle parameters on the fatigue life of parts manufactured from PLA filament using the FDM additive manufacturing method were investigated through rotary bending fatigue tests. The study established two levels (20 mm/s and 80 mm/s) for printing speed and five levels (0°, 30°, 45°, 60°, and 90°) for raster angles. Accordingly, a total of 10 distinct types of specimens were manufactured based on a full factorial experimental design. Three

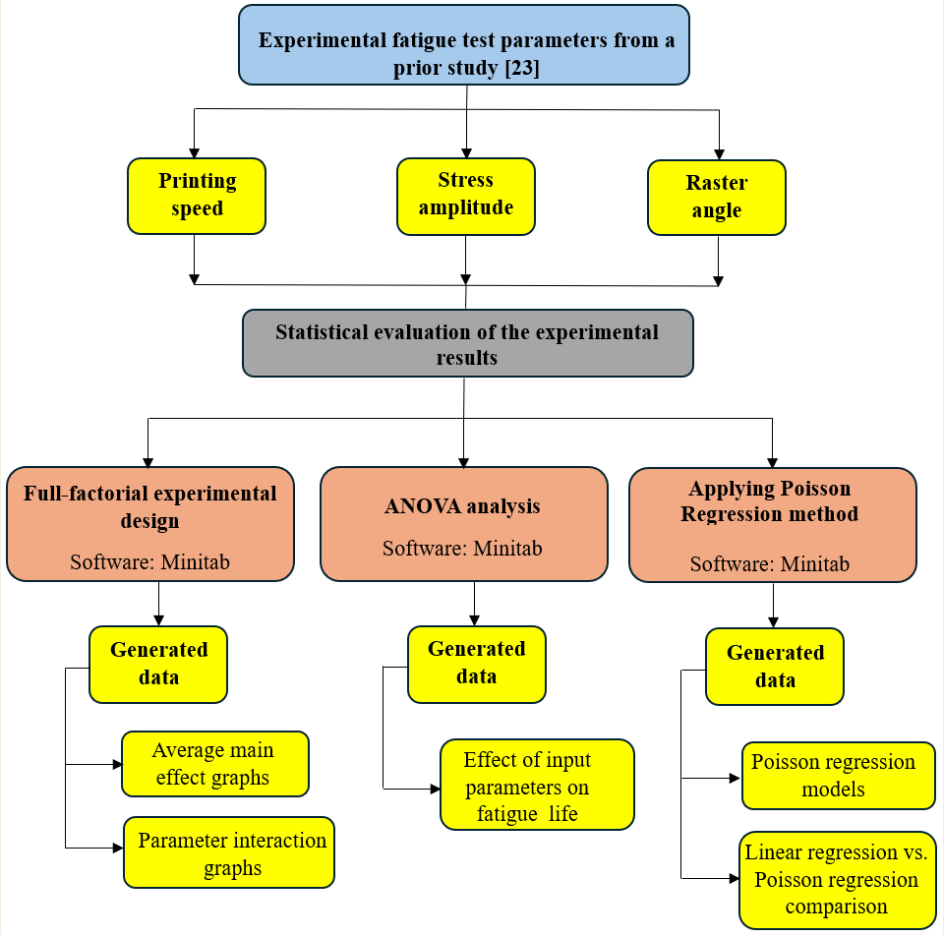

Figure 1. Flowchart diagram of the study

different stress amplitudes (9.13, 13.69, 18.25) were applied to each specimen to determine the number of cycles to failure. Subsequently, using the experimental data, stress amplitude-life (S-N) curves for each specimen type were obtained through linear regression. At the end of the study, the maximum fatigue life was found for specimens produced at a printing speed of 20 mm/s and a raster angle of 30°.

In this study, experimental data from the research by Horasan and Sarac were used to analyze the effect of test parameters on fatigue life through statistical methods, and the S-N slopes of specimen types were determined using the Poisson regression method (▶**Figure 1**).

2. Material and Methods

In this study, the experimental data obtained in the previous research and presented in ▶**Table 1** were analyzed statistically using Minitab software. The statistical analysis was conducted in three main stages. First, mean effect and parameter effect graphs were generated. In the second stage, an ANOVA table was created. In the third stage, S-N curves were produced according to the sample types based on the Poisson regression method using the experimental data.

To obtain the mean effect and parameter interaction graphs, the full-factorial experimental design section of the Minitab program was utilized. Since the experimental study conducted by Horasan and Sarac [23] followed the full-factorial experimental design, ▶**Table 2** displays the parameters and levels of the experimental study.

The effect of the factors selected for the experiment on the results is determined by analysis of variance (ANOVA), and the effect ratio of the factors on the result is calculated.

Table 1. Number of cycles to failure of the fatigue test specimens at various printing speeds, stress amplitudes, and raster angles [23].

Test Number	Printing Speed (mm/s)	Stress Amplitude (MPa)	Raster Angle	Number of Cycles to Failure (N_f)
1	20	9.13	0°	323265
2	20	9.13	30°	368202
3	20	9.13	45°	120418
4	20	9.13	60°	353938
5	20	9.13	90°	101668
6	20	13.69	0°	98292
7	20	13.69	30°	95108
8	20	13.69	45°	61306
9	20	13.69	60°	85808
10	20	13.69	90°	64051
11	20	18.25	0°	39814
12	20	18.25	30°	44906
13	20	18.25	45°	41464
14	20	18.25	60°	46580
15	20	18.25	90°	38764
16	80	9.13	0°	149021
17	80	9.13	30°	228751
18	80	9.13	45°	95334
19	80	9.13	60°	204320
20	80	9.13	90°	70142
21	80	13.69	0°	77106
22	80	13.69	30°	99897
23	80	13.69	45°	63200
24	80	13.69	60°	98456
25	80	13.69	90°	48010
26	80	18.25	0°	34622
27	80	18.25	30°	36355
28	80	18.25	45°	36986
29	80	18.25	60°	38174
30	80	18.25	90°	29818

Table 2. Experimental factors and their levels [23]

Factor	Levels	Values
Printing Speed (mm/s)	2	20; 80
Stress Amplitude (MPa)	3	9.13; 13.69; 18.25
Raster Angle (°)	5	0; 30; 45; 60; 90

3. Results and Discussion

3.1. Optimization of Experimental Results

In ▶**Figure 2**, the effect of the input parameters (print speed, stress amplitude, and raster angle) on the output parameter (number of cycles to failure) is displayed in the average main effect graph. Analyzing ▶**Figure 2** reveals that, in general, all input parameters influence the results. However, the effect of stress amplitude on fatigue strength is greater compared to the other parameters. The optimal parameters for fatigue life are a combination of a 20 mm/s print speed, 9.13 MPa stress amplitude, and a 30° raster angle. Additionally, the maximum number of cycles to failure was achieved with these parameters in experiment number 2, as shown in ▶**Table 1**. The graph in ▶**Figure 2** indicates that better results are obtained at a 20 mm/s printing speed; furthermore, the ideal raster angles for fatigue specimens are 30° and 60°, while fatigue life is negatively impacted at 45° and 90° raster angles.

▶**Figure 3** illustrates the parameter interaction graphs. In these graphs, straight lines indicate no interaction. Sloped lines indicate significant interaction effects among the factors. Upon analyzing ▶**Figure 3**, it becomes clear that substantial interactions exist among the parameters. However, the interactions between the 13.69 and 18.25 MPa stress levels with raster angle and print speed are negligible. Particularly at the 18.25 MPa stress level, it is evident that changes in raster angle and compression speed have minimal impact on the number of cycles to failure. Examination of the column graphs from the experimental results displayed in ▶**Figure 4** and ▶**Figure 5** reveals that the effect of changing the raster angle on the number of cycles to failure at 13.69 and 18.25 MPa stress levels is significantly lower compared to the 9.13 MPa stress level.

3.2. Analysis of variance (ANOVA)

Using the experimental results, the ANOVA table presented in ▶**Table 3** was created for the number of cycles to failure. ▶**Table 3** illustrates the effect ratios of the experimental parameters on the outcome (number of cycles to failure). ANOVA analysis was conducted at a 95% confidence level and a 5% significance level [24, 25]. This indicates that the most influential factor on the results is the stress level, with an effect rate of 54.93%. The effect rate of raster angle was 14.52%, while the effect rate of printing speed was 4.19%. The significance of control factors in ANOVA is determined

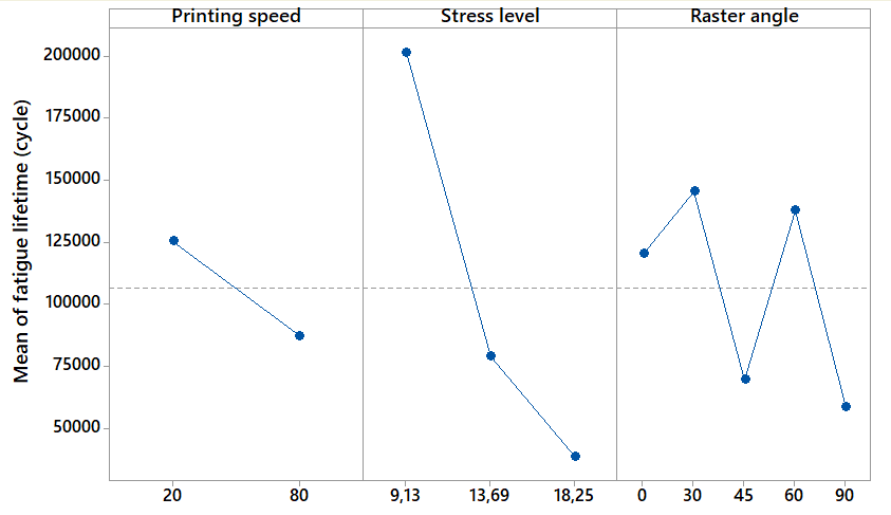

Figure 2. Main effects plots of printing parameters on fatigue life

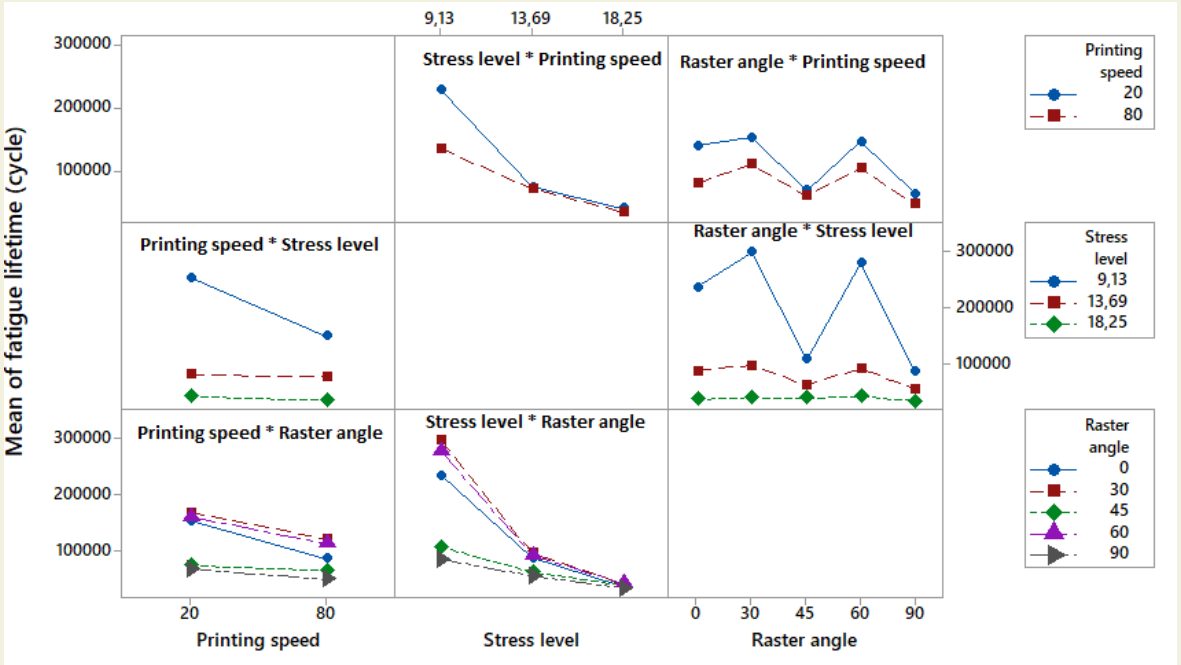

Figure 3. Effect of input parameters (printing speed, stress level, and raster angle) on fatigue lifetime

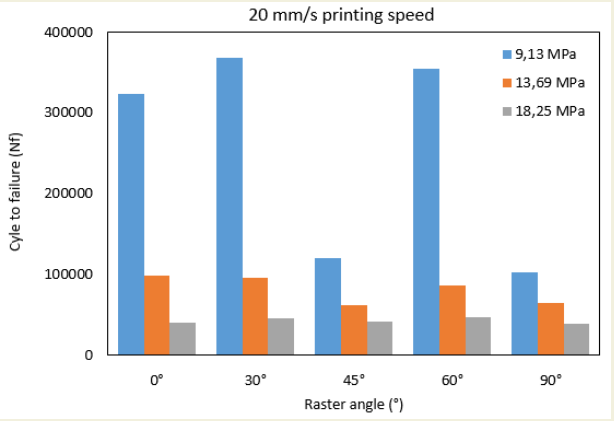

Figure 4. Failure load variations concerning raster angle and stress at a printing speed of 20 mm/s

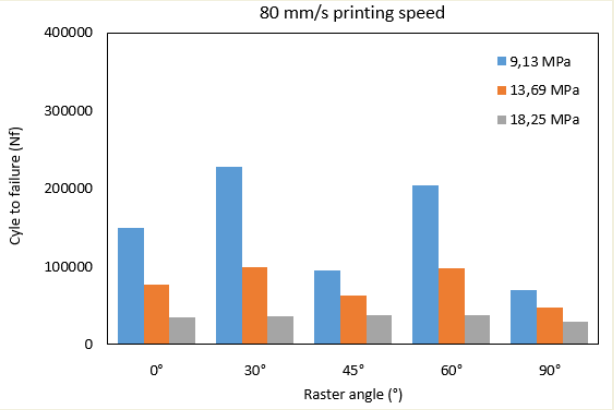

Figure 5. Failure load variations concerning raster angle and stress at a printing speed of 80 mm/s

by the P value of each factor. According to the established significance level (5%), a P value less than 0.05 signifies statistically significant results. Upon examining ▶**Table 3**, it is observed that the P values calculated for stress level and raster angle are both less than 0.05. Therefore, the stress level and raster angle parameters resulted in statistically significant changes for the number of cycles to failure. While the P value for print speed exceeds 0.05, the contribution rate of 4.19% indicates that it has the potential to influence the results.

3.3. Generating S-N Graphs Using Poisson Regression

Regression analysis models and analyzes the relationship between a dependent variable and independent variables. Horasan and Sarac [23] identified 10 types of fatigue specimens in their study. They applied stress amplitudes of 18.25, 13.69, and 9.13 MPa to each specimen type and obtained the number of cycles to failure and S-N graphs based on these experimental data. In this study, using data from the fatigue tests, the relationship between fatigue life and stress amplitude for each specimen type was modeled using the Poisson regression method. The Poisson regression model function is presented in Equation (1). The regression models generated for the specimen types are listed in ▶**Table 4**.

$$N_f = \exp\left(A - BS_a\right) \tag{1}$$

In Equation (1), N_f represents the number of cycles to failure, S_a denotes the stress amplitude applied to the

Table 3. ANOVA table for the number of cycles to failure

Source	DF	Seq SS	Contribution	Adj SS	Adj MS	F-Value	P-Value
Printing Speed	1	1.09592E+10	4.19%	1.09592E+10	1.09592E+10	3.50	0.075
Stress Level	2	1.43659E+11	54.93%	1.43659E+11	7.18294E+10	22.92	0.000
Raster Angle	4	3.79754E+10	14.52%	3.79754E+10	0.94938E+10	3.03	0.039
Error	22	6.89472E+10	26.36%	6.89472E+10	0.31339E+10	-	-
Total	29	2.61541E+11	100.00%	-	-	-	-

Table 4. Regression equations for the sample types

Sample type		Poisson regression model	R^2 Poisson regression	R^2 Lineer regression[23]
Printing speed (mm/s)	Raster angle	Nf (cyles) = exp(Y')		
20	0°	Y' = 14.8677 - 0.240353 x S_a (MPa)	99.58%	84.20%
20	30°	Y' = 15. 0999 – 0.252858 x S_a (MPa)	98.40%	79.80%
20	45°	Y' = 12.7904 - 0.122308 x S_a (MPa)	98.09%	73.10%
20	60°	Y' = 15.0297 - 0.250432 x S_a (MPa)	97.13%	78.10%
20	90°	Y' = 12.4923 - 0.105016 x S_a (MPa)	99.94%	71.40%
80	0°	Y' = 13.3490 - 0.156231 x S_a (MPa)	99.71%	96.20%
80	30°	Y' = 14.1364 - 0.195505 x S_a (MPa)	99.71%	87.00%
80	45°	Y' = 12.4059 - 0.101644 x S_a (MPa)	99.43%	95.60%
80	60°	Y' = 13.8600 - 0.177202 x S_a (MPa)	99.49%	90.40%
80	90°	Y' =12.0111 - 0.092265 x S_a (MPa)	99.57%	86.60%

specimens during fatigue tests, and *A* and *B* are the material constants. These constants are determined for each specimen type presented in ▶**Table 4**. To demonstrate the compatibility of Poisson regression models with experimental results, R^2 values were calculated and displayed in ▶**Table 4**. Additionally, the R^2 values computed using the linear regression model in the study by Horasan and Sarac [23] are also included in ▶**Table 4**. Based on the R^2 values, it is notable that the Poisson regression model aligns more closely with the experimental results. Accordingly, S_a-N_f graphs of the specimen types were created using the experimental and modeled data obtained at the end of the study (linear regression and Poisson regression models) (▶**Figures 6-10**). The S_a-N_f plots are presented in two separate figures for comparison. For instance, the S_a-N_f graphs shown in ▶**Figure 6** display the effect of a raster angle of 0° on fatigue life separately at printing speeds of 20 mm/s and 80 mm/s.

4. Conclusion

In this study, the experimental data obtained from rotary bending fatigue tests conducted by Horasan and Sarac [23], using FDM-3D printed PLA fatigue specimens, were statistically analyzed, and S-N graphs were plotted based on the Poisson regression method. The general results obtained at the end of the study are listed below:

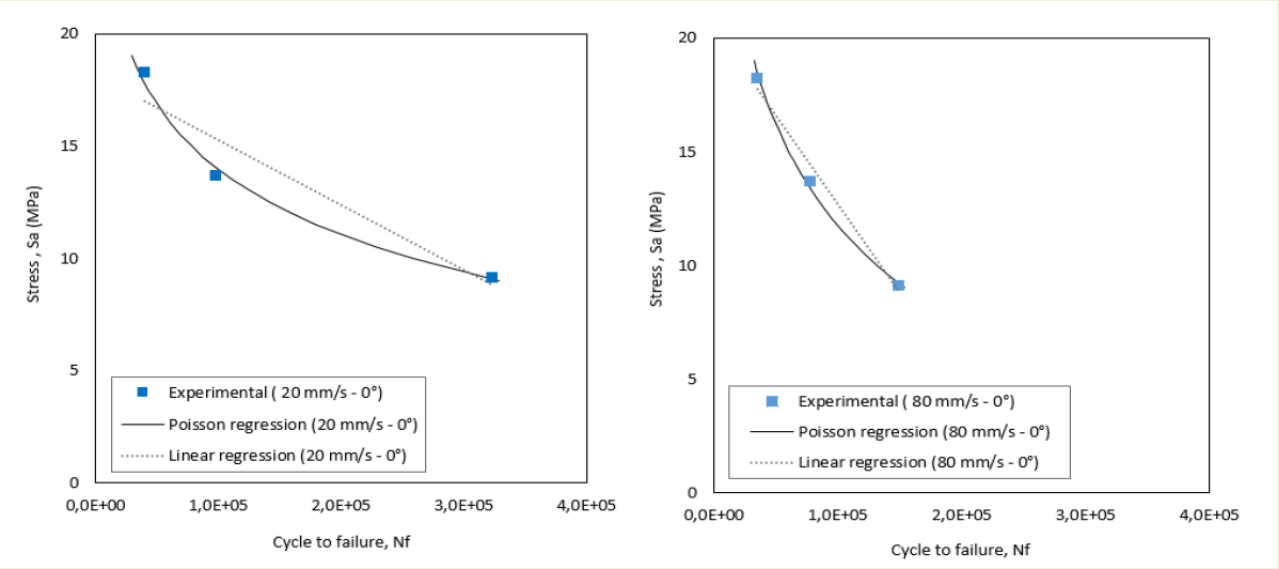

Figure 6. S_a-N_f diagrams at printing speeds of 20 mm/s and 80 mm/s at a 0° raster angle

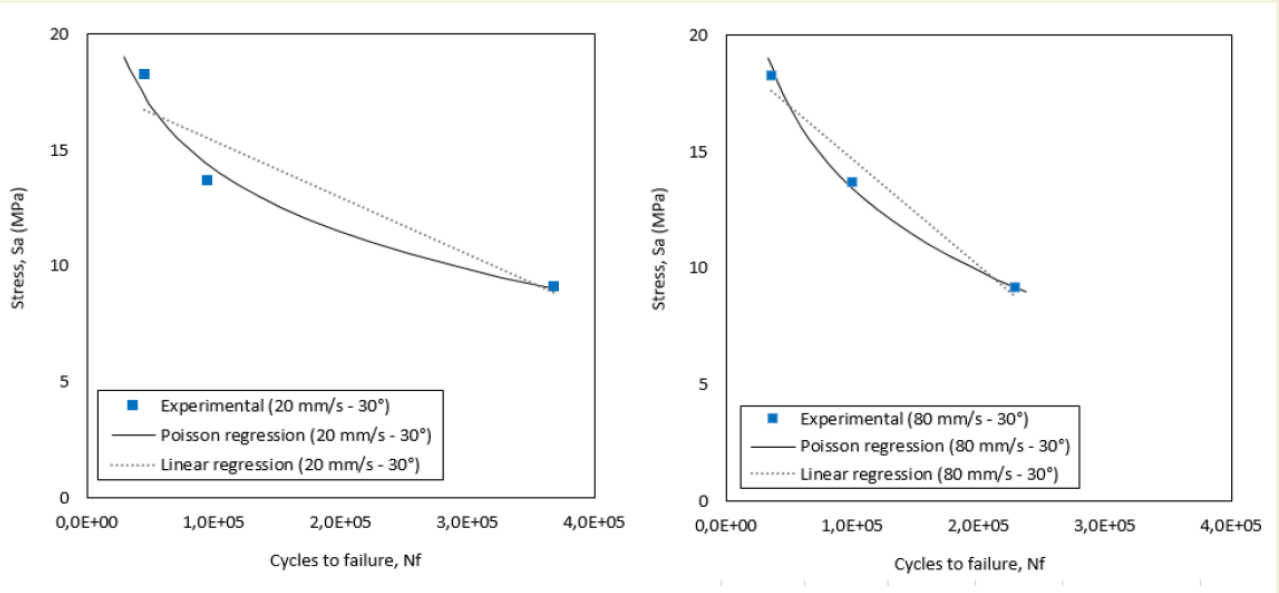

Figure 7. Sa-Nf diagrams at printing speeds of 20 mm/s and 80 mm/s at a 30° raster angle

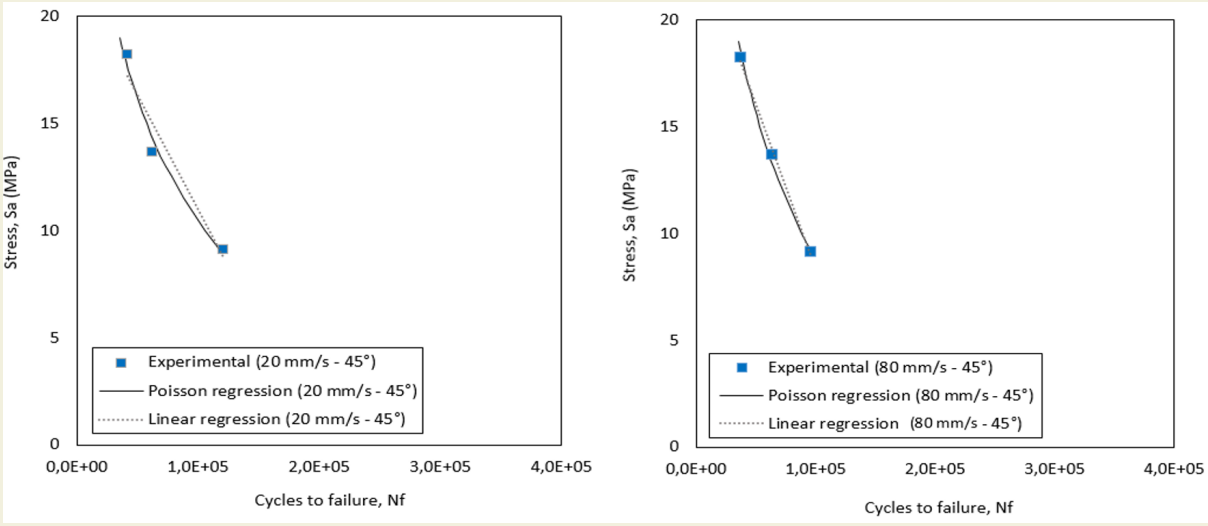

Figure 8. S_a-N_f diagrams at printing speeds of 20 mm/s and 80 mm/s at a 45° raster angle

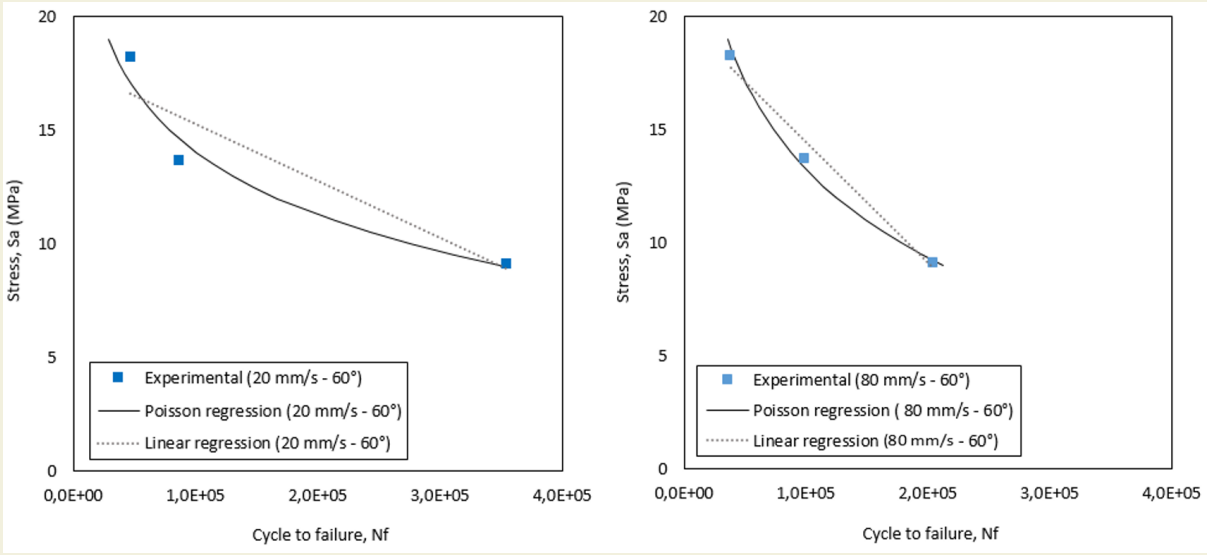

Figure 9. S_a-N_f diagrams at printing speeds of 20 mm/s and 80 mm/s at a 60° raster angle

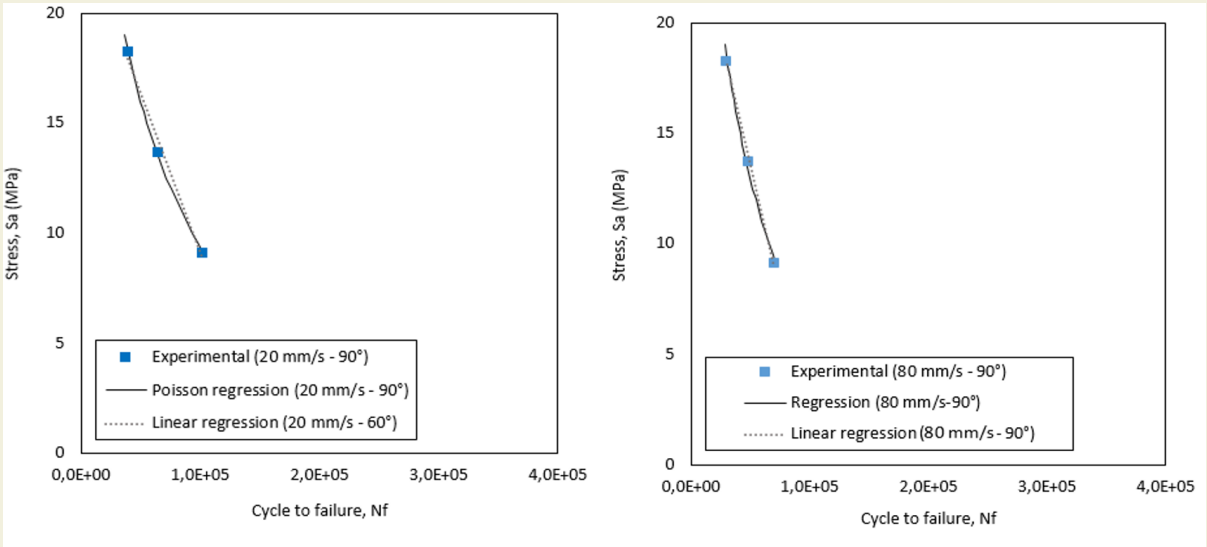

Figure 10. S_a-N_f diagrams at printing speeds of 20 mm/s and 80 mm/s at a 90° raster angle

- It was observed that the most significant parameter affecting the number of cycles to failure was the stress level. While the influence of PLA specimen production parameters (raster angle and printing speed) on the results was statistically significant at the low stress level of 9.13 MPa amplitude, at the high stress amplitude of 18.25 MPa, variations in fatigue life among the specimen types was quite limited.
- According to the main effect graph, the optimal parameter combination for achieving the maximum fatigue life was identified as 9.13 MPa stress amplitude, 20 mm/s press speed, and a 30° raster angle.
- While 30° and 60° raster angles were identified as the most suitable parameters regarding fatigue life, fatigue life decreased at 90° and 45° raster angles.
- The specimens produced at a 20 mm/s printing speed demonstrated a higher fatigue life.
- According to the ANOVA results, the parameter with the greatest influence on the results was the stress level, with a contribution rate of 54.93%. Raster angle and printing speed contributed 14.52% and 4.19% to the results, respectively.
- The Poisson regression method was found to be an effective tool for generating S-N graphs.

Research ethics

Not applicable.

Artificial Intelligence Use

The authors declare that no generative artificial intelligence (e.g., ChatGPT, Gemini, Copilot, etc.) was used in any part of this study.

Author contributions

Conceptualization: [Murat Horasan], Methodology: [Murat Horasan, İsmail Saraç], Formal Analysis: [Murat Horasan], Investigation: [Murat Horasan, İsmail Saraç], Resources: [Murat Horasan, İsmail Saraç], Data Curation: [Murat Horasan, İsmail Saraç], Writing - Original Draft Preparation: [Murat Horasan, İsmail Saraç], Writing - Review & Editing: [Murat Horasan], Visualization: [Murat Horasan, İsmail Saraç], Supervision: [Murat Horasan], Project Administration: [Murat Horasan]

Competing interests

The authors state no conflict of interest.

Research funding

None declared.

Data availability

The raw data can be obtained on request from the author.

Peer-review

Peer-reviewed by external referees.

Orcid

Murat Horasan https://orcid.org/0000-0002-7870-1486
İsmail Saraç https://orcid.org/0000-0001-8438-2744

References

[1] Harding, A., Pramanik, A., Basak, A.K., Prakash, C., & Shankar, S. (2023). Application of additive manufacturing in the biomedical field-A review. Annals of 3D Printed Medicine, 10, 100110. https://doi.org/10.1016/j.stlm.2023.100110.

[2] Salifu, S., Desai, D., Ogunbiyi, O., & Mwale, K. (2022). Recent development in the additive manufacturing of polymer-based composites for automotive structures—a review. The International Journal of Advanced Manufacturing Technology, 119, 6877–6891. https://doi.org/10.1007/s00170-021-08569-z.

[3] Singh, S., & Ramakrishna, S. (2017). Biomedical applications of additive manufacturing: Present and future. Current Opinion in Biomedical Engineering, 2, 105–115. https://doi.org/10.1016/j.cobme.2017.05.006.

[4] Tepylo, N., Huang, X., & Patnaik, P.C. (2019). Laser-Based Additive Manufacturing Technologies for Aerospace Applications. Advanced Engineering Materials, 21, 1900617. https://doi.org/10.1002/adem.201900617.

[5] Trevisan, F., Calignano, F., Aversa, A., Marchese, G., Lombardi, M., Biamino, S., Ugues, D., & Manfredi, D. (2018). Additive manufacturing of titanium alloys in the biomedical field: processes, properties and applications. Journal of Applied Biomaterials & Functional Materials, 16(2), 57–67. https://doi.org/10.5301/jabfm.5000371.

[6] Wazeer, A., Das, A., Sinha, A., Inaba, K., Ziyi, S., & Karmakar, A. (2023). Additive manufacturing in biomedical field: a critical review on fabrication method, materials used, applications, challenges, and future prospects. Progress in Additive Manufacturing, 8, 857–889. https://doi.org/10.1007/s40964-022-00362-y.

[7] Adin, M. Ş., & Kam, M. (2024). An overview of post-processing of fused deposition modelling 3D printed products. Post-Processing of Parts and Components Fabricated by Fused Deposition Modeling, 1-10.

[8] Mallikarjuna, B., Bhargav, P., Hiremath, S., Jayachristiyan, K.G., & Jayanth, N. (2025). A review on the melt extrusion-based fused deposition modeling (FDM): background, materials, process parameters and military applications. International Journal on Interactive Design and Manufacturing, 19, 651–665. https://doi.org/10.1007/s12008-023-01354-0.

[9] Sapkota, A., Ghimire, S.K., & Adanur, S. (2024). A review on fused deposition modeling (FDM)-based additive manufacturing (AM) methods, materials and applications for flexible fabric structures. Journal of Industrial Textiles, 54. https://doi.org/10.1177/15280837241282110.

[10] Solomon, I.J., Sevvel, P., & Gunasekaran, J. (2021). A review on the various processing parameters in FDM. Materials Today Proceedings, 37(2), 509–514. https://doi.org/10.1016/j.matpr.2020.05.484.

[11] Doshi, M., Mahale, A., Singh, S.K., & Deshmukh, S. (2022). Printing parameters and materials affecting mechanical properties of FDM-3D printed Parts: Perspective and prospects. Materials Today Proceedings, 50(5), 2269–2275. https://doi.org/10.1016/j.matpr.2021.10.003.

[12] Kristiawan, R.B., Imaduddin, F., Ariawan, D., Ubaidillah, & Arifin, Z. (2021). A review on the fused deposition modeling (FDM) 3D printing: Filament processing, materials, and printing parameters. Open Engineering, 11(1), 639–649. https://doi.org/10.1515/eng-2021-0063.

[13] Ahmad, M.N., & Yahya, A. (2023). Effects of 3D Printing Parameters on Mechanical Properties of ABS Samples. Designs, 7(6), 136. https://doi.org/10.3390/designs7060136.

[14] Hsueh, M.-H., Lai, C.-J., Wang, S.-H., Zeng, Y.-S., Hsieh, C.-H., Pan, C.-Y., & Huang, W.-C. (2021). Effect of Printing Parameters on the Thermal and Mechanical Properties of 3D-Printed PLA and PETG, Using Fused Deposition Modeling. Polymers, 13(11), 1758. https://doi.org/10.3390/polym13111758.

[15] Lokesh, N., Praveena, B.A., Reddy, J.S., Vasu, V.K., & Vijaykumar, S. (2022). Evaluation on effect of printing process parameter through Taguchi approach on mechanical properties of 3D printed PLA specimens using FDM at constant printing temperature. Materials Today Proceedings, 52(3), 1288–1293. https://doi.org/10.1016/j.matpr.2021.11.054.

[16] Popescu, D., Zapciu, A., Amza, C., Baciu, F., & Marinescu, R. (2018). FDM process parameters influence over the mechanical properties of polymer specimens: A review. Polymer Testing, 69, 157–166. https://doi.org/10.1016/j.polymertesting.2018.05.020.

[17] Sagias, V.D., Giannakopoulos, K.I., & Stergiou, C. (2018). Mechanical properties of 3D printed polymer specimens. Procedia Structural Integrity, 10, 85–90. https://doi.org/10.1016/j.prostr.2018.09.013.

[18] Afrose, M.F., Masood, S.H., Iovenitti, P., Nikzad, M., & Sbarski, I. (2016). Effects of part build orientations on fatigue behaviour of FDM-processed PLA material. Progress in Additive Manufacturing, 1, 21–28. https://doi.org/10.1007/s40964-015-0002-3.

[19] Saraç, İ., & Horasan, M. (2024). The Torsional Characterization of 3D-Printed Polylactic Acid Parts With Alternating Additive Manufacturing Parameters. Polymers for Advanced Technologies, 35, e6642. https://doi.org/10.1002/pat.6642.

[20] Azadi, M., Dadashi, A., Dezianian, S., Kianifar, M., Torkaman, S., & Chiyani, M. (2021). High-cycle bending fatigue properties of additive-manufactured ABS and PLA polymers fabricated by fused deposition modeling 3D-printing. Forces in Mechanics, 3, 100016, 2021. https://doi.org/10.1016/j.finmec.2021.100016.

[21] Dadashi, A., & Azadi, M. (2023). Experimental bending fatigue data of additive-manufactured PLA biomaterial fabricated by different 3D printing parameters. Progress in Additive Manufacturing, 8, 255–263. https://doi.org/10.1007/s40964-022-00327-1.

[22] Akhoundi, B., & Behravesh, A.H. (2019). Effect of Filling Pattern on the Tensile and Flexural Mechanical Properties of FDM 3D Printed Products. Experimental Mechanics, 59, 883–897. https://doi.org/10.1007/s11340-018-00467-y.

[23] Horasan, M., & Sarac, I. (2024). The fatigue responses of 3D-printed polylactic acid (PLA) parts with varying raster angles and printing speeds. Fatigue & Fracture of Engineering Materials & Structures, 47(10): 3693-3706. https://doi.org/10.1111/ffe.14406.

[24] Adin M. Ş. (2024). Experimental research of the influence of fiber laser machining parameters on HAZ width in AISI 4140 steels, Dicle University Journal of Engineering, 15(4), 873–880. https://doi.org/10.24012/dumf.1563430.

[25] Adin, M. Ş. (2024). Investigation of the effects of laser power and gas pressure on the top and bottom HAZ widths in AISI 1040 steels. Journal of Science, Technology and Engineering Research, 5(2), 163-175. https://doi.org/10.53525/jster.1583593